

Accounts

Multi-Stage Amphoteric Redox Hydrocarbons Based on a Phenalenyl Radical

Kazuhiro Nakasuji* and Takashi Kubo

Department of Chemistry, Graduate School of Science, Osaka University, Toyonaka, Osaka 560-0043

Received April 9, 2004; E-mail: Nakasuji@chem.sci.osaka-u.ac.jp

Molecular design and properties of amphoteric redox hydrocarbons are reviewed. Our molecular design is based on a phenalenyl radical, which has a non-bonding molecular orbital with an occupation number of one and is known to behave as a two-stage amphoteric redox system. We have prepared eight amphoteric redox compounds containing two or three phenalenyl units. Cyclic voltammetry showing small E_1^{sum} values confirms the high amphotericity of these compounds. The properties of ionic redox species generated are also investigated. At the last part of this account, we show some aspects of a singlet biradicaloid character that originates from a small HOMO–LUMO gap.

Molecular design and synthesis of the redox systems giving stable redox species and showing high redox ability are important themes of fundamental chemistry. We have concentrated on the multi-stage amphoteric redox hydrocarbons that are easily oxidized and reduced by multi-stage electron transfer. In principle, the ultimate material that exhibits the highest amphotericity is graphite,[1] which is known to be a good electroconductive material. Thus the molecules with a high amphotericity, i.e., a small HOMO–LUMO gap, are attractive components of molecular metals. The synthesis and the conductive properties of the molecular metals having a small HOMO–LUMO gap have already been reported by some groups.[2] These conductive single molecules generally contain metal and hetero atoms such as sulfur and nitrogen. We have attempted to produce hydrocarbon metals, which would be one of the ultimate targets of molecular metals.[3] Although the electro-conductivity of the designed molecules is the most important property, our interests are primarily in the establishment of molecular design strategies so as to exhibit high amphotericity and in the elucidation of the mechanisms of the high amphotericity. A special issue is the molecular design of the molecules with an extremely small HOMO–LUMO gap, i.e., biradicaloid character in the ground state.

Our common molecular design is based on the phenalenyl radical **1**•, which is known to behave as a two-stage amphoteric redox hydrocarbon (Chart 1). We have designed and synthesized eight amphoteric redox molecules containing phenalenyl units.

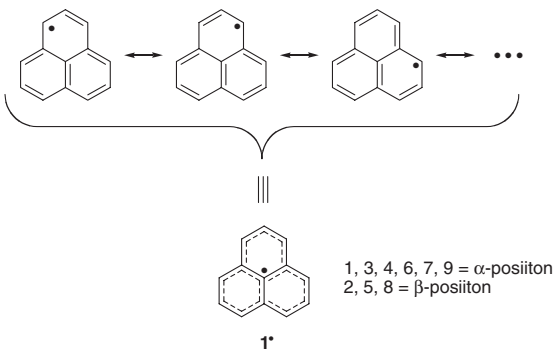

1•

Chart 1.

Molecular Design

Some conjugated hydrocarbons are known to exhibit the amphoteric redox property that a molecule is oxidized and reduced by multi-stage electron transfer. The numerical sum of oxidation potential (E^{ox}) and reduction potential (E^{red}), i.e., $E^{sum} = E^{ox} + (-E^{red})$, might be used to evaluate the amphoteric redox abilities of a given molecule, the amphotericity.[1] A compound with low ionization potential and high electron affinity, i.e., high HOMO and low LUMO, will show highly amphoteric redox ability to give stable redox states. For hydrocarbon-based amphoteric redox compounds, degenerated HOMO and LUMO with β coefficient of zero will lead to the highest amphotericity in the simple HMO framework. Such a molecular orbital with an energy of $\alpha + 0\beta$ is generally referred to as a non-bonding molecular orbital (NBMO). Addition or removal of electrons in NBMO should not change the magnitude of π-electron delocalization energy in the simple HMO approximation level. Thus a compound with NBMO as a frontier orbital will be a potential candidate to exhibit the highest redox ability.[3] A representative is phenalenyl radical **1**•, which has NBMO with an occupation number of one (Fig. 1). This radical exhibits a E_1^{sum} value of 1.6 V, which is relatively small among hydrocarbons. Although three redox states (**1**$^+$,

Published on the web October 9, 2004; DOI 10.1246/bcsj.77.1791

1•, and **1**$^-$) of phenalenyl species are known to be relatively stable and their properties have been investigated in detail,[4] the open-shell phenalenyl radical suffers from a serious disadvantage, i.e., the lack of kinetic stability. Phenalenyl radical tends to dimerize or to give oxidized species in the presence of air like ordinary radicals. In principle, there are two approaches for building stable amphoteric redox molecules retaining the high redox ability of phenalenyl species: 1) kinetic stabilization or thermodynamic stabilization of open-shell molecules by introducing some bulky substituents or by delocalizing unpaired electron over a wide range of the molecule; 2) connection of two phenalenyl radicals with a π-conjugated systems to produce closed-shell molecules.

The second type of approach is the most fascinating molecular design because of a wide selection of conjugated systems available as a connector. Figure 2 illustrates an example of the intermolecular perturbation of two phenalenyl units by connecting with ethene to give 1,2-bis(phenalen-1-ylidene)ethane (BPLA, **2**, Chart 2). The two active molecular orbitals, Ψ'_S and Ψ'_A, of two phenalenyl units arranged in symmetric and antisymmetric manner are written as

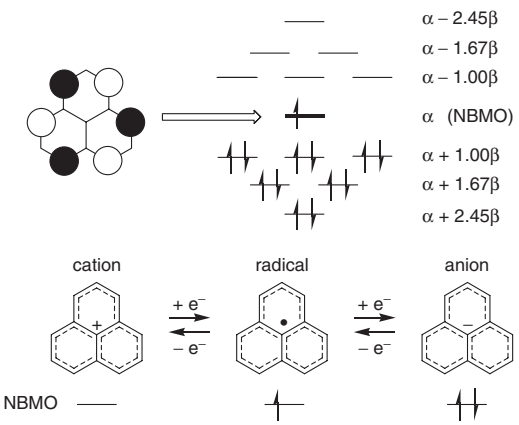

Fig. 1. Molecular orbitals of phenalenyl radical **1**• calculated by the HMO method.

$$\Psi'_S = 2^{-1/2}(\varphi + \varphi') \quad (1)$$

$$\Psi'_A = 2^{-1/2}(\varphi - \varphi') \quad (2)$$

where φ and φ' are singly occupied molecular orbitals (SOMOs) of each phenalenyl radical. These newly formed active MOs are nearly degenerate. By symmetry, Ψ'_S nteracts with the symmetric molecular orbital Ψ''_S of ethene, which has bonding character. Similarly, Ψ'_A interacts with the antisymmetric molecular orbital Ψ''_A of ethene. On the basis of the perturbation theory, HOMO (Ψ_A) and LUMO (Ψ_S) of BPLA will consist mainly of Ψ'_A and Ψ'_S with a little Ψ''_A and Ψ''_S, respectively. This prediction is easily justified by a simple Hückel molecular orbital (HMO) calculation. Figure 3

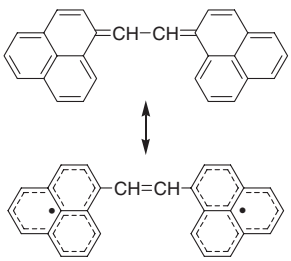

BPLA, **2**

Chart 2.

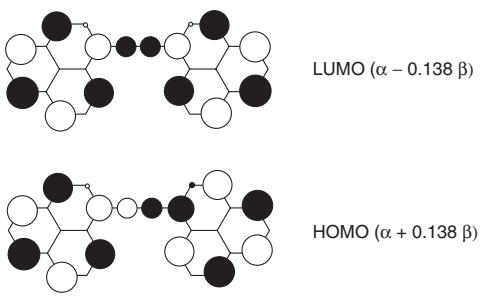

Fig. 3. HOMO and LUMO of BPLA **2**.

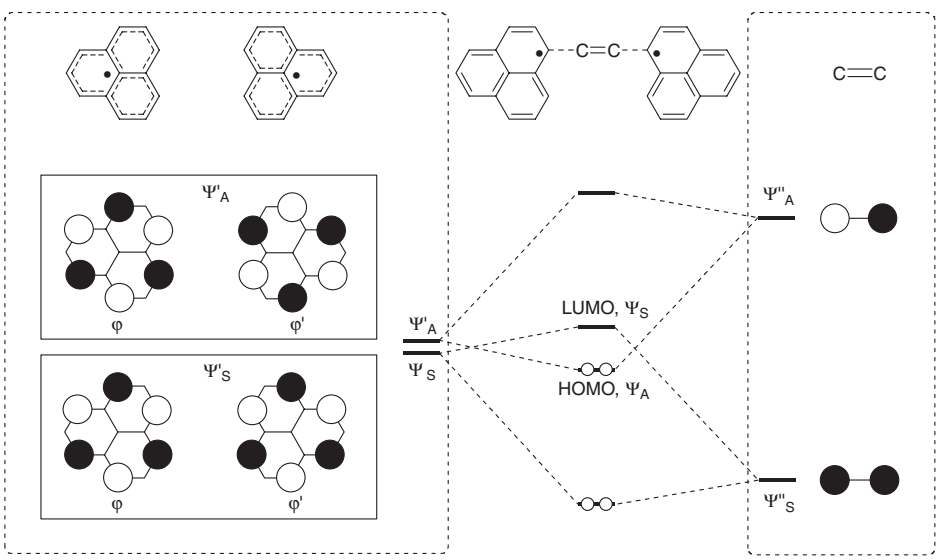

Fig. 2. Perturbative interaction of phenalenyl radicals with ethene.

shows frontier orbitals of BPLA calculated by the HMO method. Molecular orbitals distribute mainly on phenalenyl units (~90%) in a similar pattern of NBMO of phenalenyl. An in-phase connection between Ψ'_A and Ψ''_A leads to bonding interaction to give an orbital energy of $\alpha + 0.138\beta$. Similarly, an out-of-phase interaction between Ψ'_S and Ψ''_S affords an anti-bonding orbital Ψ_S of $\alpha - 0.138\beta$. For interaction between $\Psi'_{S,A}$ and $\Psi''_{S,A}$, the magnitude of the change in orbital energy is given by $E = a^2b^2\beta^2/[E(\Psi'_{S,A}) - E(\Psi''_{S,A})]$, where a and b are atomic orbital coefficients of $\Psi'_{S,A}$ and $\Psi''_{S,A}$ at linking sites, respectively. Because the highly delocalized SOMO in **1**• leads to a small value of a ($\pm 1/\sqrt{6}$), the numerator is relatively small. Additionally, the denominator will be large because the $\Psi'_{S,A}$ always possesses non-bonding character (i.e., $E(\Psi'_{S,A}) = \alpha$) and conjugated systems as a connector usually have well-separated bonding and anti-bonding MOs. As a result, the perturbation of the $\Psi'_{S,A}$ with $\Psi''_{S,A}$ is small and the molecule tends to show relatively small HOMO–LUMO splitting. Thus BPLA should behave as an amphoteric redox molecule with the character of a phenalenyl radical.

One Phenalenyl System: Chemistry of 2,5,8-Tri-*tert*-butylphenalenyl Radical

Before discussing about well-designed amphoteric redox compounds, we will summarize the chemistry of phenalenyl species briefly.

Historical Overview of Phenalenyl Species. The parent phenalenyl radical **1**• has not been isolated and exists only in solution. The radical **1**• was first generated by air oxidation of phenalenyl anion $\mathbf{1}^-$[5,6] and was also observed in the reaction of phenalene **3** with air[7] or quinones (Chart 3).[8] Another approach was seen in the references that described the equilibrium reaction between **1**• and σ-dimer **4**.[5,9] Thermodynamic stability of **1**• can be estimated from bond dissociation energy of phenalene **3** (270 kJ/mol), which is one of the weakest C–H bonds among closed-shell hydrocarbons.[10] The bond dissociation enthalpy of σ-dimer **4** is also found to have a small value of 41 kJ/mol (in toluene) and 47.5 kJ/mol (in CCl_4).[11] NMR spectra, useful for evaluation of aromaticity and charge distribution, are generally not informative for radicals because of signal broadening. The most powerful method to investigate the properties of radicals is electron spin resonance (ESR) spectroscopy. This method is widely applied to many phenalenyl radical derivatives including deuterium and ^{13}C labeled compounds.[7,9,12] ESR spectrum of **1**• consists of seven principal lines, each of which is further split into quartet lines. The hyperfine coupling constants are 0.63 and 0.18 mT, respectively. The splitting pattern and larger coupling constants at α-positions show that **1**• retains highly symmetric structure D_{3h} and that unpaired electrons mainly distribute over α-positions.

Phenalenyl cation $\mathbf{1}^+$ was first generated by the reaction of chloro compound with silver perchlorate.[13] Hydride abstraction of phenalene **3** by triphenylmethyl cation or quinones also affords the cation $\mathbf{1}^+$.[14] This cation readily decomposes in moist air but can be stored under N_2 atmosphere without changes. For relatively stable carbocations, pK_{R^+} is commonly used to measure the stability of the species. Although experimental determination of pK_{R^+} for $\mathbf{1}^+$ has not been achieved due to irreversible disproportionation of 1-phenalenol, pK_{R^+} value of $\mathbf{1}^+$ is estimated to be 0–2 based on the HMO calculation.[15] ^1H NMR spectrum of $\mathbf{1}^+$ gives two signals at δ 9.30 (6H) and 8.48 (3H).

Phenalenyl anion $\mathbf{1}^-$ was generated by the treatment of phenalene **3** with phenyllithium[16] or potassium methoxide.[5,6] This red anion species is persistent in the condition without air and water. The ^1H NMR spectrum gives a very simple AB_2 system centered at δ 5.91 (3H) and 5.17 (6H), consistent with D_{3h} structure.[17] The thermodynamic stability of $\mathbf{1}^-$ can be estimated from the pK_a value (~18) of phenalene **3** in DMSO, which is almost identical to that of cyclopentadiene (18.0).[10]

Isolated Phenalenyl Radical. Chemistry of 2,5,8-Tri-*tert*-butylphenalenyl Radical 5•: The first isolation of phenalenyl radical was established by introducing *tert*-butyl groups at three β-positions.[18] These bulky groups effectively protect reactive sites, i.e., six α-positions, having a large coefficient in SOMO. This protection prevents σ-bonded dimerization of **5**• even in solid state. X-ray crystal structure analysis shows that **5**• forms a π-dimer in an arrangement where intra-dimer SOMO–SOMO overlap is effectively maximum (Chart 4). Large antiferromagnetic intermolecular exchange interaction ($2J/K_b = -2000$ K) in the dimer pair suggests a singlet biradical ground state for the dimer.[19] CP/MAS ^{13}C NMR spectroscopy gives no appreciable amount of paramagnetic shifts and peak broadening, giving strong evidence of singlet character. Recent quantum chemical calculations reveal that the SOMO–SOMO overlap effect would be responsible for the strong antiferromagnetic interaction.[20] The intra-dimer interaction is also found in characteristic optical transitions in solid state. The solid-state electronic spectrum affords a broad and intense absorption centered at 612 nm, which is not observed

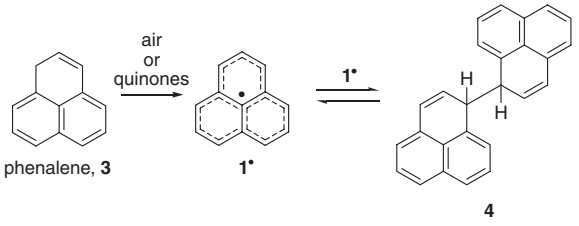

Chart 3.

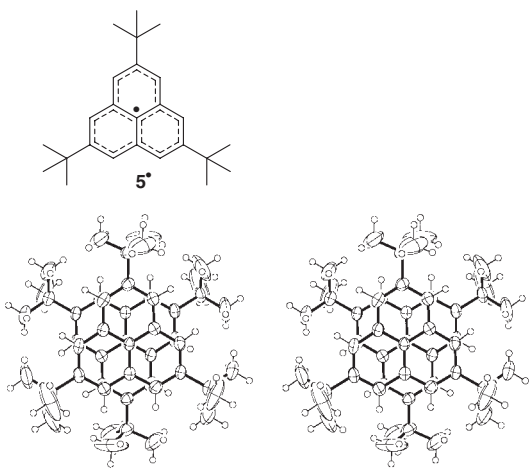

Chart 4.

in solution. The transition moment of the band is polarized along the direction connecting the center of the phenalenyl rings. This finding suggests that the origin of the band may be an electronic transition between HOMO and LUMO in the dimeric pair newly formed by the orbital interaction of a pair of SOMOs in **5**•. In solution, the dimer of **5**• almost completely dissociates into the monomer at room temperature. On cooling, the monomer gradually associates to form the dimer.[21] The ESR spectrum of the monomer shows a dominant septet hyperfine structure with a coupling constant of 0.62 mT.[18]

Redox species of **5**• were easily generated and were found to be persistent in non-aerial conditions.[18] Cation species $\mathbf{5}^+$ was obtained as red crystals by the reaction of tri-*tert*-butylphenalene **6** with triphenylmethyl cation in CH_2Cl_2. The cation holds almost planar phenalenyl ring and no dimerization are found by the preliminary X-ray crystal structure analysis. The pK_{R^+} of $\mathbf{5}^+ \cdot SbCl_6^-$ is determined to be 1.5–1.6 by spectrophotometric titration. The cyclic voltammogram of the cation gives two reversible redox waves at +0.27 and −1.26 V vs SCE, which are corresponding to E^{ox} and E^{red} of **5**•, respectively. The E^{sum} value of 1.53 V is similar to that of the parent phenalenyl radical **1**•.[22] The reversibility is consistent with the stability and isolability of the radical **5**• and also suggests the possibility to isolate anion species $\mathbf{5}^-$. The anion $\mathbf{5}^-$ was generated from **6** by treatment of potassium hydride in DME in a sealed degassed tube to give red columnar crystals. However, attempted operation for X-ray crystal structure analysis has failed even in argon atmosphere, probably because of trace amounts of oxygen. ^{1}H NMR spectra have one resonance for ring protons at δ 9.24 for $\mathbf{5}^+$ and δ 5.33 for $\mathbf{5}^-$ as a singlet.

Two-Phenalenyl System: Closed-Shell Amphoteric Redox Molecules

Ethene and Acetylene Bridged System. Early development of amphoteric redox hydrocarbon has been carried out by the group of Hünig.[23] The basic structure is composed of a cross-conjugated polyene such as **7**–**9** (Chart 5). These molecules are designed so that charges can delocalize over terminal cyclohexadinenylidene units in redox states (Scheme 1). Similarly, our designed amphoteric redox compound BPLA **2** is

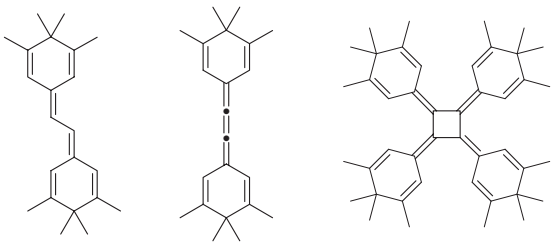

Chart 5.

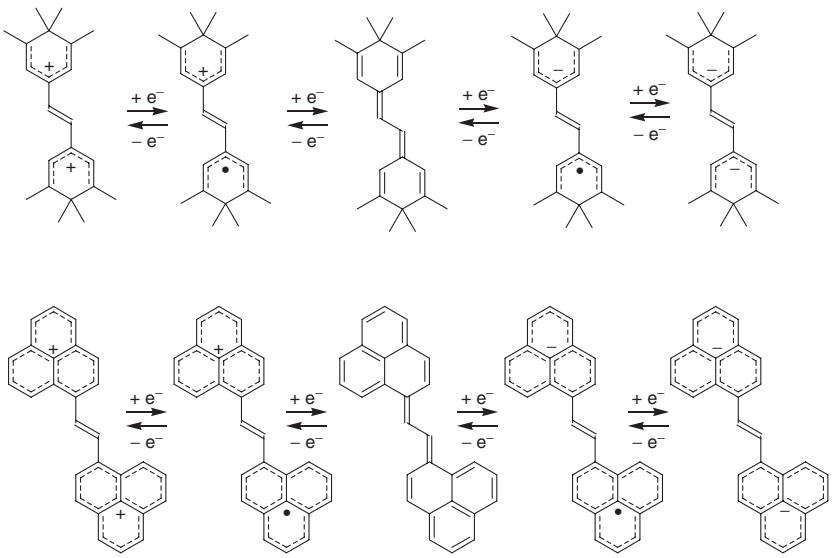

Scheme 1.

Table 1. Electrochemical Data of Amphoteric Redox Compounds (V vs SCE)

	E_3^{ox}	E_2^{ox}	E_1^{ox}	E_1^{red}	E_2^{red}	E_3^{red}	E_1^{sum}	E_2^{sum}	E_3^{sum}
Phenalenyl, **1**•			+0.7	−0.9			1.6		
TTB-Phen, **5**•			+0.27	−1.26			1.53		
BPLA, **2**		+0.83	+0.39	−1.12	−1.35		1.51	2.18	
BPLE, **10**		+0.78	+0.51	−0.83	−1.21		1.34	1.99	
PDPL, **11**		+1.02	+0.56	−0.43	−1.17		0.99	2.19	
DIP-IDPL, **12b**		+0.84	+0.62	−0.48	−1.07		1.10	1.91	
TTB-IDPL, **12c**		+0.84	+0.48	−0.67	−1.25		1.15	2.09	
TTB-TDPL, **14b**		+0.94	+0.47	−0.53	−0.90		1.00	1.84	
HTB-TBzD, **13b**•	+0.87	+0.68	+0.27	−0.51	−0.89	−1.25	0.78	1.57	2.12

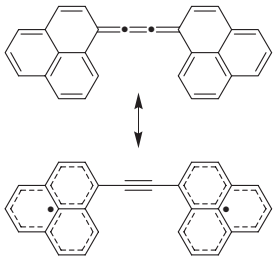

BPLE, **10**

Chart 6.

expected to behave like an example of Hünig's system. In the case of **2**, phenalenyl cation and anion structures appear in the redox states, as shown in Scheme 1.[24] More highly delocalized structure in redox states of **2** would lead to lower E^{ox} and higher E^{red} values, in comparison with **7** (Table 1). The electrochemical data obtained by cyclic voltammetry show a smaller ${E_1}^{sum}$ value for **2** than that for **7**. Clearly, such a small ${E_1}^{sum}$ value observed in **2** can be attributed to the considerable electronic stability of the three redox states of the phenalenyl moiety.

Such success in finding a design to enhance amphotericity prompted us to extend our idea to the related system, 1,2-bis-(phenalen-1-ylidene)ethene (BPLE, **10**, Chart 6) in which two phenalenyl moieties are connected with two sp-carbon atoms.[25] BPLE **10** gives a lower-energy transition at 720 nm than BPLA **2** (704 nm), suggesting a smaller HOMO–LUMO gap of **10**. Positive shifts of the first oxidation and reduction potentials are presumably attributable to the difference in electro-negativity between sp- and sp^2-hybridized carbons. The larger shift of ${E_1}^{red}$ compared to ${E_1}^{ox}$ leads to smaller ${E_1}^{sum}$ values in **10**, which is consistent with the UV/vis spectra.

Polycyclic Conjugated System. New molecular designs are demanded for further enhancement of the amphotericity. The ${E_1}^{sum}$ value is a measure of the equilibrium constants K_1 for the following reaction.

$$\mathbf{X}^+ + \mathbf{X}^- \overset{K_1}{\rightleftharpoons} 2\mathbf{X} \tag{3}$$

$${E_1}^{sum} = {E_1}^{ox} + (-{E_1}^{red}) = {E_1}^{ox} - {E_1}^{red} \tag{4}$$

$$\Delta G^\circ = -nF{E_1}^{sum} \tag{5}$$

$$K_1 = \exp(-\Delta G^\circ/RT). \tag{6}$$

The ultimate state (${E_1}^{sum} = 0$) can be established in the condition of $K_1 = 1$. In the system described above, K_1 values are much higher than unity and the neutral species **X** is much more stabilized thermodynamically compared to the redox phase. Thus stabilizing the left-hand state and/or destabilizing the right-hand state in the Eq. 3 will diminish the ${E_1}^{sum}$ value. Based on this idea, we designed a new polycyclic system PDPL **11** which contains an 8π-electron antiaromatic pentalene moiety in the center of the molecule (Chart 7).[26] The neutral state of **11** will be substantially destabilized by the electronic contribution of a pentalene system. This pentalene structure disappears in redox states with two phenalenyl systems emerging at the termini of the molecule. The CV measurement gives a very small ${E_1}^{sum}$ value (0.99 V) and the highest ${E_1}^{red}$ (−0.43 V). In contrast to PDPL, peropyrene, which

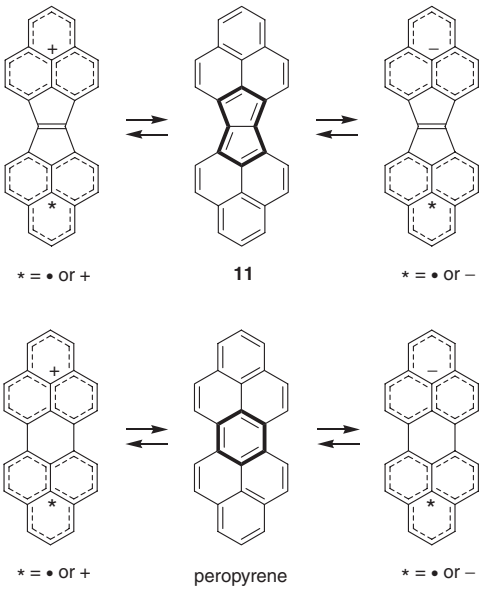

Chart 7.

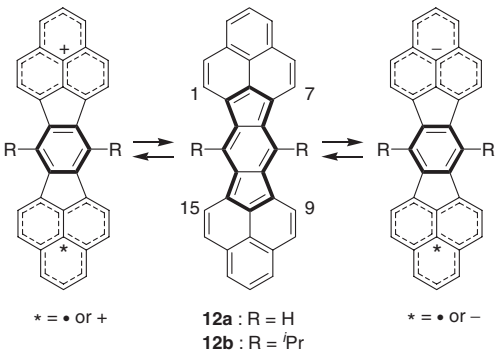

Chart 8.

bears phenalenyl moieties but acquires aromatic-stabilization of a central benzene ring, shows a very large ${E_1}^{sum}$ value of 2.29 V. The ${E_1}^{red}$ value of PDPL is comparable to that of well-known electron acceptors, 1,4-benzoquinone (${E_1}^{red} = -0.38$ V) and 1,2-naphthoquinone (${E_1}^{red} = -0.46$ V). Such a highly electron-donating and -accepting character for **11** implies the bi-functionality, so that this hydrocarbon behaves as a donor with one molecule and as an acceptor with another. PDPL **11** formed 1:1 complexes with 2,4,7-trinitrofluorenone and TCNQ. However, no CT-complexes were obtained with donors so far.

The more expanded conjugation system IDPL **12a** contains 12π-electron *s*-indacene in the center of the molecule (Chart 8). Similar to PDPL **11**, the neutral **12a** will be destabilized by the unfavorable $4n\pi$ electronic contribution of *s*-indacene unit. A major difference of molecular design between **11** and **12a** can be seen in the redox states, in which the central benzene structure is formed in addition to two terminal phenalenyl units. Because parent **12a** was not soluble in common organic solvents, bulky isopropyl groups were introduced at the central benzene ring.[27] The ${E_1}^{sum}$ value of **12b** is found to be very small but is slightly greater than that of **11**. However, the ${E_2}^{sum}$ value of **12b** is smaller than that of **11**. This high-

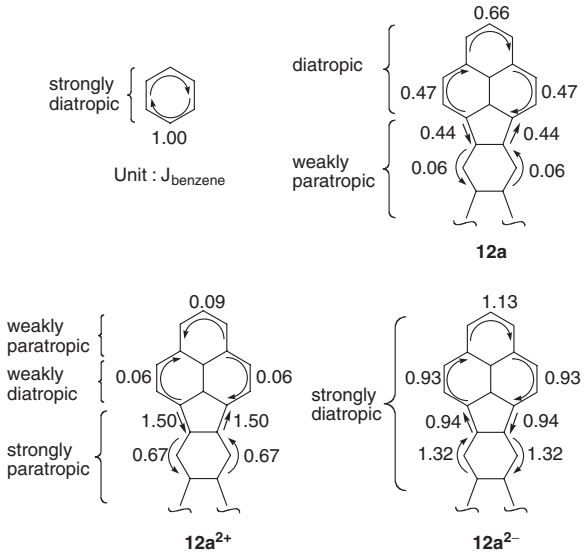

Fig. 4. Ring current calculation of **12a**, **12a**$^{2+}$, and **12a**$^{2-}$.

ly amphoteric redox character makes it possible to generate doubly-charged species **12b**$^{2+}$ and **12b**$^{2-}$. These super-charged species can be observed by ^{1}H NMR with no difficulties. The most striking feature is anomalous lower-field shifts found in isopropyl and 1,7,9,15-position protons of **12b**$^{2-}$ in spite of the shielding effect derived from negative charges. These protons appear at lower-fields than the corresponding protons of **12b**$^{2+}$, in spite of the negative charge shielding. The London–McWeeny ring current calculation reasonably accounts for the unexpected shielding (Fig. 4). The calculation predicts the strongly diatropic ring current on the periphery of the molecules in **12a**$^{2-}$, whereas a strongly paratropic ring current would be induced around the *s*-indacene unit in **12a**$^{2+}$.

Kinetically Stabilized Amphoteric Redox System. The primary interest of potentially amphoteric redox compounds is evaluation of the magnitude of E_1^{sum} value. Another prominent feature is that these compounds will expectedly give stable reduced and oxidized species. As described above, amphoteric redox compounds indeed show small E_1^{sum} values and give some redox species. However, some irreversible redox waves observed in these compounds imply the lack of sufficient persistency to investigate the detailed electronic structure of redox species. Furthermore, the neutral compounds also suffer from oxidation in air. One of the most rational methods to increase kinetic stability is the introduction of bulky substituents at the reactive site.

TTB-IDPL **12c** is one such case (Chart 9).[28] Great enhancement of the kinetic stability resulted in no remarkable decomposition in air during more than one year. The cyclic voltammogram affords fully reversible redox waves, as shown in Fig. 5. The persistency of the neutral and redox states enables to analyze the electronic structure in detail. The radical cation **12c**$^{\bullet+}$ was easily generated by the reaction of **12c** with $SbCl_5$ and was found to be stable at room temperature. The radical anion **12c**$^{\bullet-}$ was obtained by the treatment of **12c** with a potassium mirror in THF. Although any contact of this anion with air results in immediate decomposition, **12c**$^{\bullet-}$ is persistent in sealed degassed tube even at room temperature. Both

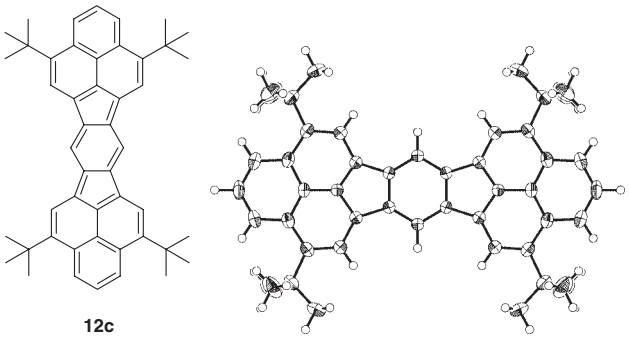

Chart 9.

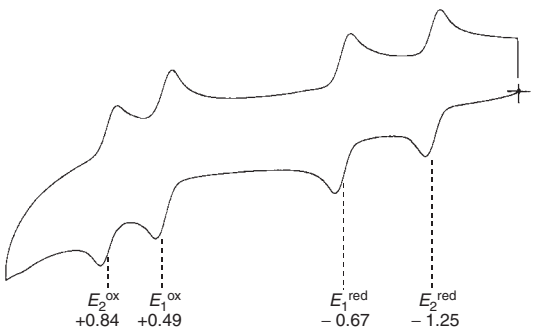

Fig. 5. Cyclic voltammogram of **12c**.

radical species give rise to the intense ESR signals with no detectable changes in the range of 213–273 K. Based on the experimental and theoretical hyperfine coupling constants, the unpaired electron is not confined to one limited phenalenyl unit but is delocalized over the entire molecule. The delocalization of spin is confirmed by the UV/vis/NIR spectra. Both radical species afford very low-energy optical transitions in the NIR region with vibrational structures. These NIR bands are assignable to the transitions of SOMO (ψ_{16}) $\rightarrow$ LUMO (ψ_{17}) for **12c**$^{\bullet+}$ and HOMO (ψ_{16}) $\rightarrow$ SOMO (ψ_{17}) for **12c**$^{\bullet-}$, and are well reproduced in energy on the basis of the INDO/S CI calculation, which shows highly delocalized electronic structures for **12c**$^{\bullet+}$ and **12c**$^{\bullet-}$. The well-resolved NIR bands imply that these low-energy absorptions are not due to an intra- or inter-molecular CT transition. These findings support the idea that formula A is a better description for the mono-valent paramagnetic species **12c**$^{\bullet+}$ and **12c**$^{\bullet-}$ than formula B which describes the spin and charge localization on each phenalenyl ring (Chart 10).

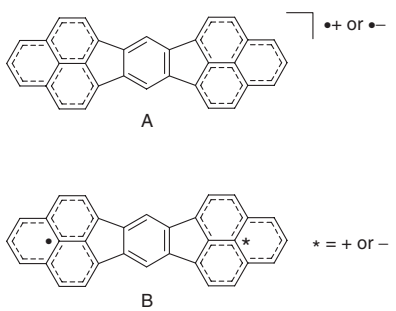

Chart 10.

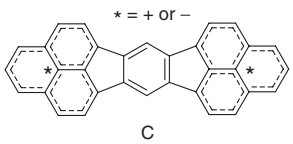

Chart 11.

The HMO–McLachlan spin density calculation indicates that 86% of the π-spin density resides on the two phenalenyl units in **12c**$^{\bullet+}$ and **12c**$^{\bullet-}$ with the similar spin distribution pattern to that of phenalenyl radical. The large spin density and the similarity of the distribution patterns on two phenalenyl units support the idea that both HOMO and LUMO of **12c** should have a large extent of an NBMO character that originats from non-bonding character of SOMO in phenalenyl radical. Thus, the small E_1^{sum} value of **12c** can be attributed to the NBMO character of the frontier orbitals.

Discussions about the density and distribution pattern of spin for **12c**$^{\bullet+}$ and **12c**$^{\bullet-}$ can be applied to discussions of charges for divalent species **12c**$^{2+}$ and **12c**$^{2-}$. The ^{13}C NMR spectroscopy is widely used to estimate the charge density for closed shell ionic species. Dication species **12c**$^{2+}$ was obtained as a purple solution by dissolving **12c** in concentrated D_2SO_4, whereas treatment of the dihydro derivative of **12c** with a potassium mirror in THF yielded dianion **12c**$^{2-}$ in a sealed degassed tube. Both species are persistent even at room temperature. The divalent species show minor differences in ^{13}C chemical shifts compared to the shifts for the corresponding carbon atoms of phenalenyl cation and anion, indicating that the charges are delocalized mainly over the two phenalenyl units. The HMO calculation indicates that two phenalenyl units have 91% of the total positive charges and 81% of the total negative charges in **12a**$^{2+}$ and **12a**$^{2-}$, respectively. Thus, formula C largely contributes to the electronic structure of the divalent species (Chart 11).

Three-Phenalenyl System: A Highly Delocalized Open-Shell Molecule

As described above, an open-shell molecular design based on NBMO is very fascinating because of the essential ease of addition or removal of electrons. The problem for the instability that originates from an unpaired electron will be overcome by the high delocalization of the spin. TBzD **13a**$^{\bullet}$ containing three phenalenyl units will show the delocalization of an unpaired electron over the whole of the molecule (Chart 12).[29] Simple HMO calculation of **13a**$^{\bullet}$ presents degenerate MOs in frontier orbitals $\psi_{22} \sim \psi_{24}$. The presence of the degenerate MOs constitutes a feature of TBzD **13a**$^{\bullet}$ (Fig. 6).

Kinetically stabilized **13b**$^{\bullet}$ gave six reversible one-electron redox waves as shown in Fig. 7. This behavior provides evidence for the formation of the stable mono-, di-, tri-valent species. To the best of our knowledge, only a few examples are known of compounds that exhibit six-stage amphoteric redox behavior (Chart 13). Furthermore, the E_1^{sum} value of **13b**$^{\bullet}$ is substantially smaller than those reported so far for hydrocarbons.

The neutral radical **13b**$^{\bullet}$ is expected to be stable due to kinetic stabilization of *t*-butyl groups and thermodynamic stabilization of spin delocalization. Although **13b**$^{\bullet}$ can be purified

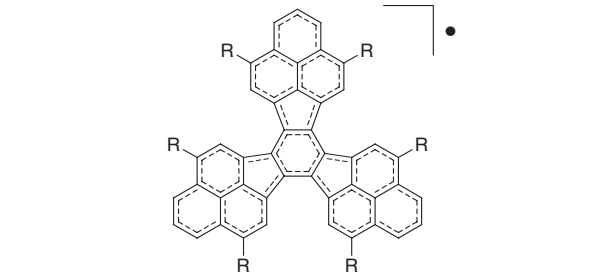

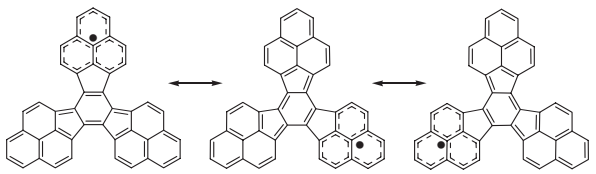

Chart 12.

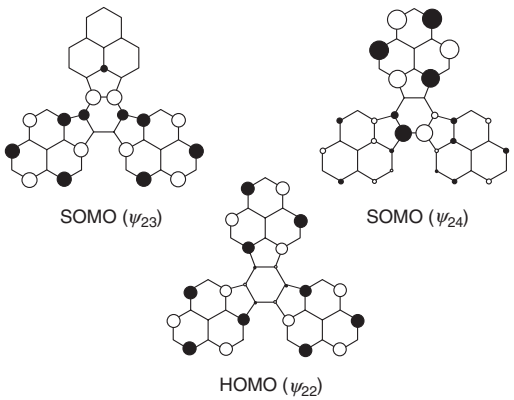

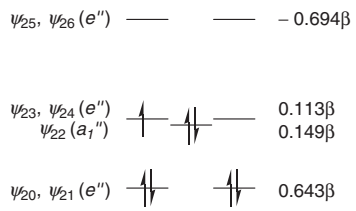

Fig. 6. Selected molecular orbitals of **13a**$^{\bullet}$ calculated by the HMO method.

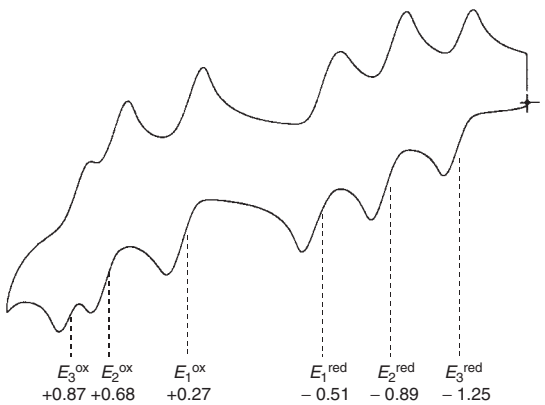

Fig. 7. Cyclic voltammogram of **13b**$^{\bullet}$.

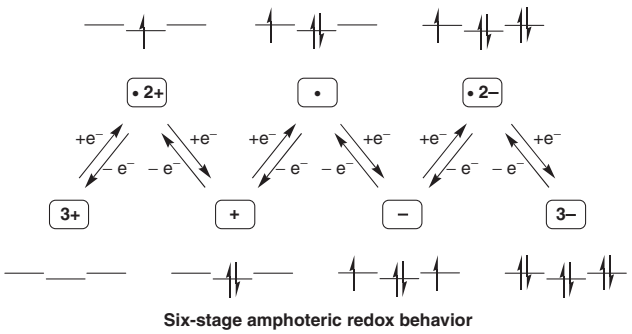

Chart 13.

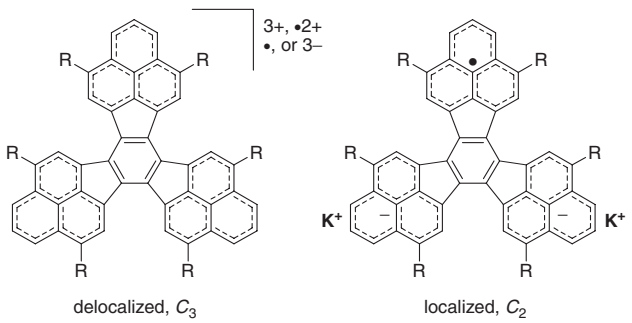

Chart 14.

by column chromatography, exposure to air leads to decomposition in a day. According to the HMO calculation, one electron occupies a pair of the degenerate MOs ψ_{23} and ψ_{24}. This gives rise to a degenerate $^2E_1''$ state, which should distort away from C_3 symmetry to C_2 form by the Jahn–Teller effect. However, the spin density of **13b•** estimated from the ESR spectra is consistent with the spin delocalization on the entire C_3 symmetric molecule (Chart 14).

Monoradical dication **13b**$^{\bullet 2+}$ should have a non-degenerate SOMO (ψ_{22}) with C_3 symmetric MO distribution pattern. The ESR spectrum of **13b**$^{\bullet 2+}$ supports this highly delocalized structure of the spin. On the other hand, the pair of the relevant frontier orbitals of monoradical dianion **13b**$^{\bullet 2-}$ is degenerate or nearly degenerate, with an occupancy number of three. The ESR spectrum of **13b**$^{\bullet 2-}$ reveals that the unpaired electron mainly localizes on one phenalenyl unit. This Jahn–Teller distortion would be caused by ion pairing of the counter cations K^+ which might reside near two phenalenyl units.

The prime interest in monoanion **13b**$^-$ relates to whether this species will be singlet or triplet. ESR measurements afford no signal attributable to a triplet species in the samples at 77 K and 173 K. Although the absence of the triplet ESR signals does not prove the singlet ground state of **13b**$^-$, ion pairing of K^+ should be responsible for this spin multiplicity of **13b**$^-$.

The terminal states in the amphoteric redox system of **13b•** are trication **13b**$^{3+}$ and trianion **13b**$^{3-}$ species. Both supercharged states are generated with no difficulties and are persistent in sealed degassed tubes even at room temperature. ^{1}H NMR gives very simple patterns consistent with the C_3 symmetry structure. The stability of **13b**$^{3+}$ and **13b**$^{3-}$ originates from phenalenyl cation and anion structure, which is supported by ^{13}C NMR and HMO calculation results.

Biradicaloid Character Originating from Small HOMO–LUMO Gap

Most Kekulé compounds have an adequately separated HOMO–LUMO gap and their ground states are well described by a single ground state determinant $^1\Phi_0$. For compounds with a small HOMO–LUMO gap, however, such a single configuration is not adequate for the description of the ground state and one must expect an admixture of the doubly excited configuration $^1\Phi_{H,H\rightarrow L,L}$ into the ground configuration $^1\Phi_0$. In the limiting case, $^1\Phi_0$ and $^1\Phi_{H,H\rightarrow L,L}$ mix so strongly (i.e., weight of $^1\Phi_0$ and $^1\Phi_{H,H\rightarrow L,L}$ is 50:50) and the compound should possess a perfect singlet biradical character. The double excitation to LUMO also depends on an exchange interaction ($K_{H,L}$) between HOMO and LUMO.

In the case of the compound with high-lying HOMO and low-lying LUMO, its frontier orbitals will show non-bonding character. Michl used the term "π,π-biradicaloid" for the compounds which possess two approximately non-bonding π-orbitals.[30] The amphoteric redox compounds described above are designed so that the feature of phenalenyl radical is utilized effectively. The frontier orbitals on phenalenyl units of these compounds have very similar patterns to NBMO of phenalenyl radical. Thus the amphoteric redox compounds containing phenalenyl units are expected to show a biradicaloid character. TTB-IDPL **12c** would be one case. Neutral **12c** gives a simple ^{1}H NMR spectrum consistent with the molecular framework with D_{2h} symmetry. At elevated temperature, progressive line broadening is observed, as shown in Fig. 8. ESR measurement of solid **12c** affords typical spectra for triplet species and the temperature dependence of the signal indicates the thermal excitation to the triplet state with the energy gap (ΔE_{S-T}) of 20.4 kJ/mol. The unpaired electron of the triplet species would broaden the NMR signals. Such a thermal accessibility to the triplet state suggests a small HOMO–LUMO splitting and a large exchange interaction $K_{H,L}$. On

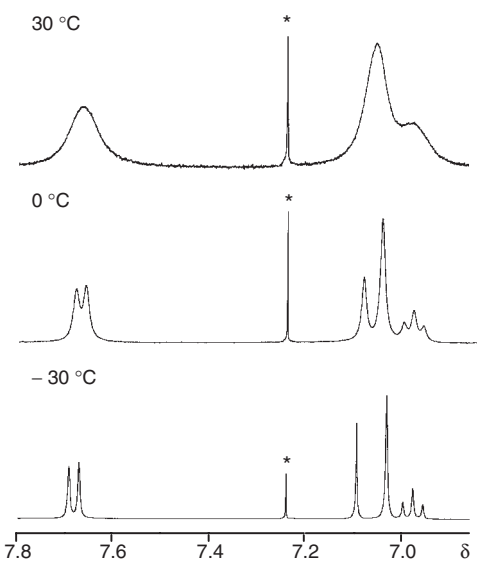

Fig. 8. Temperature dependence of ^{1}H NMR spectra of **12c** in aromatic regions. An small asterisk indicates peaks of benzene.

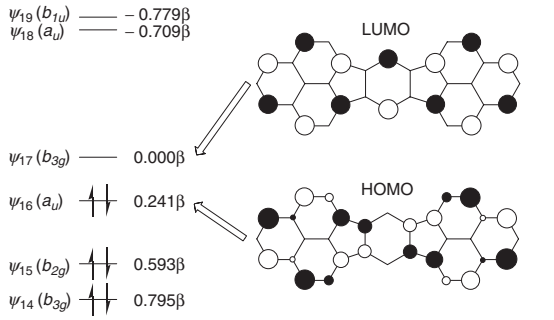

Fig. 9. Selected molecular orbitals of **12a** calculated by the HMO method.

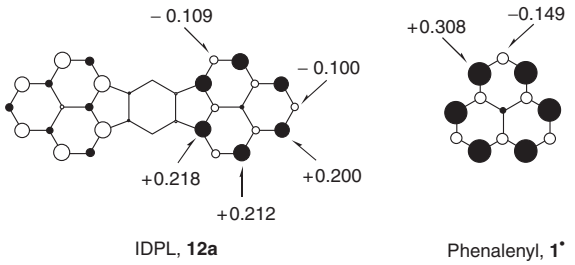

Fig. 10. Spin densities of **12a** and **1•** calculated by UB3LYP/6-31G(d,p).

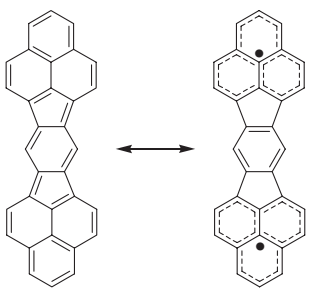

Chart 15.

the basis of the HMO calculation, the HOMO–LUMO gap of IDPL **12a** is 0.24β and a large special overlap of these frontier orbitals supports the considerable amount of $K_{H,L}$ (Fig. 9). This MO picture at Hückel level provides another fascinating property, i.e., a description of the ground state configuration. The CI calculation affords a substantial admixture (15%) of the double excitation $^1\Phi_{H,H\rightarrow L,L}$ into the ground configuration $^1\Phi_0$ at CASSCF(2,2)/6-31G(d,p) level. The singlet biradical index, proposed by Neese recently,[31] of **12a** is ~70% based on the CI calculation. The singlet biradical picture can also be obtained by the broken symmetry DFT calculation based on UB3LYP/6-31G(d,p), which indicates that ~70% of spin density of phenalenyl radical resides on each phenalenyl unit of **12a** (Fig. 10). Valence bond picture is helpful for understanding the unusual electronic structure. The Kekulé form of **12a** loses "aromatic" stabilization in the central benzene ring, whereas benzene and phenalenyl radical structure appear in biradical form of **12a** (Chart 15).

Recently, we have obtained more indicative results about singlet biradicaloid character. TTB-TDPL **14b** gave no ^{1}H NMR signals in aromatic region even at −90 °C and afford-

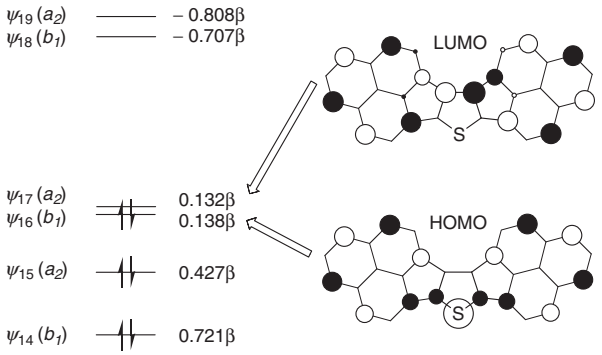

Fig. 11. Selected molecular orbitals of **14a** calculated by the HMO method.

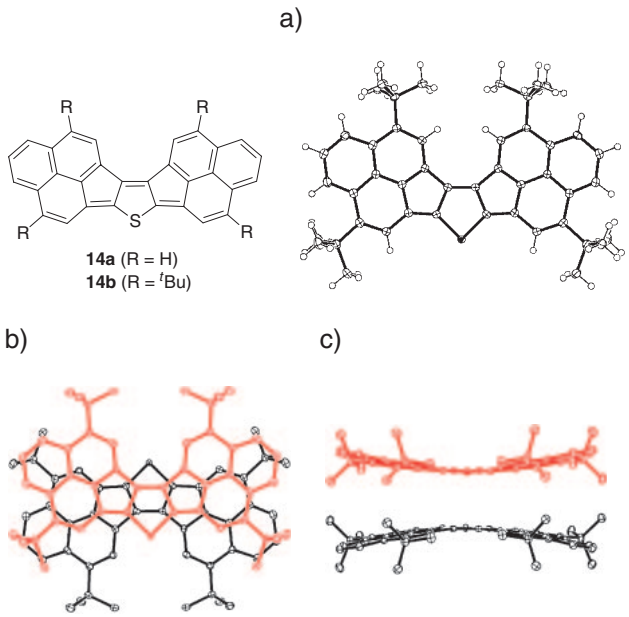

Fig. 12. Crystal structure of **14b**. a) Top view of monomer, b) top view of dimer, and c) side view of dimer.

ed ESR signals attributable to thermally excited triplet species with a small ΔE_{S-T} of ~5 kJ/mol.[32] The ΔE_{S-T} value of **14b** is smaller than that of **12b**, consistent with the trend of the E^1_{sum} values. The biradical index based on the CI calculation is 39% for **14b**. Similar to IDPL **12a**, a large $K_{H,L}$ value is expected for TDPL **14a** (Fig. 11). The crystal structure of TTB-TDPL **14b** consists of a dimer pair with a non-bonded contact of each thiophene ring in ~3.2 Å. (Fig. 12). The attractive intermolecular interaction in the dimer would arise from the double excitation configuration $^1\Phi_{H,H\rightarrow L,L}$, i.e., a singlet biradical contribution. The reaction of **14b** with TCNE exclusively affords a TCNE-adduct (Chart 16) within 10 seconds even in the dark at room temperature. NMR studies of the adduct reveal that TCNE reacted at the carbon atoms bonded to sulfur atom. Because [10 + 2] cycloaddition is generally forbidden as a thermally concerted process, the reaction would proceed through the path related to the doubly excited configuration $^1\Phi_{H,H\rightarrow L,L}$. These finding are consistent with the broken symmetry DFT calculation, which predicts a considerable amount of spin density on the thiophene ring.

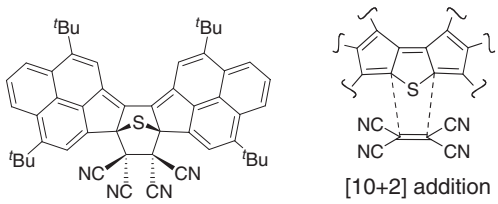

Chart 16.

Conclusion and Outlook

In this account, we summarized our work in multi-stage amphoteric redox compounds utilizing the NBMO character of phenalenyl radical. These well-designed compounds have shown both electron donor and acceptor ability and have given stable mono-, di-, and tri-valent ionic species. Such an amphoteric redox behavior will originating from an NBMO character of the frontier orbitals, which has been characterized by ESR and ^{13}C NMR measurements. The spin and charges are mainly distributed on phenalenyl moieties in a similar pattern to those of phenalenyl species. Thus the phenalenyl units contribute largely to the high amphotericity and the stability of ionic redox species.

The chemistry described in the last part of this account appears to prepare the ground for testing concepts and theories of solid state properties of conjugated singlet biradicals, such as crystal packing, magnetism, and electro-conductive behavior. Closed-shell conjugated systems based on a phenalenyl radical will lead to various conjugated biradicaloid compounds isolable in air.

We thank I. Murata for continuous guidance and helpful suggestions. We also thank K. Yamamoto for continuing interest and guidance in this work. The efforts of K. Yoshida, M. Yamaguchi, S. Sasaki, K.-U. Klabunde, T. Masui, K. Ohashi, Y. Fujiwara, M. Akabane, K. Goto, and M. Sakamoto are highly appreciated. ESR studies have been carried out in cooperation with the group of T. Takui at Osaka City University. The work cited here has been supported by Grant-in-Aid for Scientific Research on Priority Areas (No. 01648003; No. 06218217; Area No. 769, Proposal No. 15087202) from the Ministry of Education, Culture, Sports, Science and Technology (MEXT).

References

1 V. D. Parker, *J. Am. Chem. Soc.*, **98**, 98 (1976).

2 H. Tanaka, Y. Okano, H. Kobayashi, W. Suzuki, and A. Kobayashi, *Science*, **291**, 285 (2001); S. K. Pal, M. E. Itkis, R. W. Reed, R. T. Oakley, A. W. Cordes, F. S. Tham, T. Siegrist, and R. C. Haddon, *J. Am. Chem. Soc.*, **126**, 1478 (2004); X. Chi, M. E. Itkis, B. O. Patrick, T. M. Barclay, R. W. Reed, R. T. Oakley, A. W. Cordes, and R. C. Haddon, *J. Am. Chem. Soc.*, **121**, 10395 (1999); S.-L. Zheng, J.-P. Zhang, W.-T. Wong, and X.-M. Chen, *J. Am. Chem. Soc.*, **125**, 6882 (2003); Y. Yamashita and M. Tomura, *J. Mater. Chem.*, **8**, 1933 (1998); D. F. Perepichka, M. R. Bryce, A. S. Batsanov, E. J. L. McInnes, J.-P. Zhao, and R. D. Farley, *Chem.—Eur. J.*, **8**, 4656 (2002); J. Roncali, *Chem. Rev.*, **97**, 173 (1997); H. A. M. van Mullekom, J. A. J. M. Vekemans, and E. W. Meijer, *Chem.—Eur. J.*, **4**, 1235 (1998); K. Takahashi, S. Fujita, K. Akiyama, M. Miki, and K. Yanagi, *Angew. Chem., Int. Ed.*, **37**, 2484 (1998).

3 R. C. Haddon, *Nature (London)*, **256**, 394 (1975).

4 D. H. Reid, *Quart. Rev., Chem. Soc.*, **19**, 274 (1965); I. Murata, "Topics in Non-Benzenoid Aromatic Chemistry," ed by T. Nozoe, R. Breslow, K. Hafner, S. Ito, and I. Murata, Hirokawa, Tokyo (1976), Vol. 1, p. 159.

5 D. H. Reid, *Chem. Ind.*, **1956**, 1504.

6 D. H. Reid, *Tetrahedron*, **3**, 339 (1958).

7 P. B. Sogo, M. Nakazaki, and M. Calvin, *J. Chem. Phys.*, **26**, 1343 (1957).

8 D. H. Reid, M. Fraser, B. B. Molloy, H. A. S. Payne, and R. G. Sutherland, *Tetrahedron Lett.*, **15**, 530 (1961).

9 F. Gerson, *Helv. Chim. Acta*, **49**, 1463 (1966).

10 M. J. Bausch, R. Gostowski, G. Jirka, D. Selmarten, and G. Winter, *J. Org. Chem.*, **55**, 5805 (1990).

11 S. Zheng, J. Lan, S. I. Khan, and Y. Rubin, *J. Am. Chem. Soc.*, **125**, 5786 (2003).

12 R. Biehl, M. Plato, and K. Möbius, *J. Chem. Phys.*, **63**, 3515 (1975); R. Biehl, Ch. Hass, H. Kurrechk, W. Lubitz, and S. Oestreich, *Tetrahedron*, **34**, 419 (1978); W. Broser, H. Kurreck, S. Oestreich-Janzen, G. Schlömp, H.-J. Fey, and B. Kirste, *Tetrahedron*, **35**, 1159 (1979); Ch. Hass, B. Kirste, H. Kurreck, and G. Schlömp, *J. Am. Chem. Soc.*, **105**, 7375 (1983).

13 R. Pettit, *Chem. Ind.*, **1956**, 1306; R. Pettit, *J. Am. Chem. Soc.*, **82**, 1972 (1969).

14 W. Bonthrone and D. H. Reid, *J. Chem. Soc.*, **1959**, 2773; D. H. Reid and R. G. Sutherland, *J. Chem. Soc.*, **1963**, 3295.

15 D. Meuche, H. Strauss, and E. Heilbronner, *Helv. Chim. Acta*, **41**, 57 (1958).

16 V. Boekelheide and C. E. Larrabee, *J. Am. Chem. Soc.*, **72**, 1245 (1950).

17 V. Rautenstrauch and F. Wingler, *Tetrahedron Lett.*, **51**, 4703 (1965).

18 K. Goto, T. Kubo, K. Yamamoto, K. Nakasuji, K. Sato, D. Shiomi, T. Takui, M. Kubota, T. Kobayashi, K. Yakushi, and J. Ouyang, *J. Am. Chem. Soc.*, **121**, 1619 (1999).

19 K. Fukui, K. Sato, D. Shiomi, T. Takui, K. Itoh, K. Gotoh, T. Kubo, K. Yamamoto, K. Nakasuji, and A. Naito, *Synth. Met.*, **103**, 2257 (1999); K. Fukui, K. Sato, D. Shiomi, T. Takui, K. Itoh, K. Gotoh, T. Kubo, K. Yamamoto, K. Nakasuji, and A. Naito, *Mol. Cryst. Liq. Cryst. Sci. Technol.*, **334**, 49 (1999).

20 T. Takano, T. Taniguchi, H. Isobe, T. Kubo, Y. Morita, K. Yamamoto, K. Nakasuji, T. Takui, and K. Yamaguchi, *J. Am. Chem. Soc.*, **124**, 11122 (2002).

21 J.-M. Lü, S. V. Rosokha, and J. K. Kochi, *J. Am. Chem. Soc.*, **125**, 12161 (2003).

22 See for the amphoteric electrochemical behavior of hydrocarbon-based phenalenyl radicals with heteroatom substituents: K. Nakasuji, M. Yamaguchi, I. Murata, K. Yamaguchi, T. Fueno, H. Ohya-Nishiguchi, T. Sugano, and M. Kinoshita, *J. Am. Chem. Soc.*, **111**, 9265 (1989); R. C. Haddon, F. Wudl, M. L. Kaplan, J. H. Marshall, R. E. Cais, and F. B. Bramwell, *J. Am. Chem. Soc.*, **100**, 7629 (1978); P. A. Koutentis, Y. Chen, Y. Cao, T. P. Best, M. E. Itkis, L. Beer, R. T. Oakley, A. W. Cordes, C. P. Brock, and R. C. Haddon, *J. Am. Chem. Soc.*, **123**, 3864 (2001); X. Chi, M. E. Itkis, K. Kirschbaum, A. A. Pinkerton, R. T. Oakley, A. W. Cordes, and R. C. Haddon, *J. Am. Chem. Soc.*, **123**, 4041 (2001).

23 B. Hagenbruch, K. Hesse, S. Huunig, and G. Klug, *Liebigs Ann. Chem.*, **1981**, 256.

24 K. Nakasuji, K. Yoshida, and I. Murata, *J. Am. Chem. Soc.*, **104**, 1432 (1982).

25 K. Nakasuji, K. Yoshida, and I. Murata, *Chem. Lett.*, **1982**,

969.
26 K. Nakasuji, K. Yoshida, and I. Murata, *J. Am. Chem. Soc.*, **105**, 5136 (1983).
27 I. Murata, S. Sasaki, K.-U. Klabunde, J. Toyoda, and K. Nakasuji, *Angew. Chem., Int. Ed. Engl.*, **30**, 172 (1991).
28 K. Ohashi, T. Kubo, T. Masui, K. Yamamoto, K. Nakasuji, T. Takui, Y. Kai, and I. Murata, *J. Am. Chem. Soc.*, **120**, 2018 (1998).
29 T. Kubo, K. Yamamoto, K. Nakasuji, T. Takui, and I. Murata, *Angew. Chem., Int. Ed. Engl.*, **35**, 439 (1996); T. Kubo, K. Yamamoto, K. Nakasuji, T. Takui, and I. Murata, *Bull. Chem. Soc. Jpn.*, **74**, 1999 (2001).
30 J. Kolc and J. Michl, *J. Am. Chem. Soc.*, **95**, 7391 (1973).
31 D. Herebian, K. E. Wieghardt, and F. Neese, *J. Am. Chem. Soc.*, **125**, 10997 (2003).
32 T. Kubo, M. Sakamoto, M. Akabane, Y. Fujiwara, K. Yamamoto, M. Akita, K. Inoue, T. Takui, and K. Nakasuji, *Angew. Chem., Int. Ed.*, in press.

Kazuhiro Nakasuji, Professor at Osaka University, was born in Hyogo, Japan in 1941. He graduated from Osaka University in 1965 and received his Ph.D. in 1970 under the guidance of Professor Masazumi Nakagawa. He joined Professor Ichiro Murata's group at Department of Chemistry, Faculty of Science, Osaka University in 1971 as an Assistant Professor and from 1983 to 1988 as an Associate Professor. He also worked as a postdoctoral fellow at Columbia University from 1977 to 1979. He experienced being a guest scientist of Institute for Solid State Physics, the University of Tokyo in 1987. He moved to Institute for Molecular Science as a Professor in 1988. From 1993, he has been a Professor at Department of Chemistry, Faculty of Science, Osaka University (from 1996, Graduate School of Science). His research interests focus on the exploration of characteristic delocalized electronic systems based on the structural and physical organic chemistry, especially multi-stage redox systems, stable neutral radicals, proton–electron cooperative systems, and hydrogen-bonded metal complexes.

Takashi Kubo, Assistant Professor at Osaka University, was born in Yamaguchi, Japan, in 1968. He graduated from Osaka University in 1991, received M.Sc. in 1993 under the guidance of Professor Ichiro Murata, and received Ph.D. in 1996 under the guidance of Professor Kazuhiro Nakasuji. After working at Mitsubishi Chemical Co., he joined Professor Nakasuji's group at Department of Chemistry, Graduate School of Science, Osaka University in 2000 as Assistant Professor. He received the Bulletin of the Chemical Society of Japan Award in 2001. His research interests are structural and physical organic chemistry, mainly the syntheses and properties of phenalenyl-based polycyclic aromatic hydrocarbons with a small HOMO–LUMO gap, and the development of cooperative proton and electron transfer systems based on transition metal complexes.